Failure to increase glucose consumption through the pentose-phosphate pathway results in the death of glucose-6-phosphate dehydrogenase gene-deleted mouse embryonic stem cells subjected to oxidative stress

Stefania FILOSA*[1], Annalisa FICO*, Francesca PAGLIALUNGA*, Marco BALESTRIERI†, Almudena CROOKE*‡, Pasquale VERDE*, Paolo ABRESCIA*†, José M. BAUTISTA‡ and Giuseppe MARTINI*

*IGB 'Adriano Buzzati Traverso' CNR, Via G. Marconi 12, 80125 Napoli, Italy, †Dipartimento di Fiosiologia Generale ed Ambientale, Università degli Studi di Napoli Federico II, Napoli, Italy, and ‡Departamento de Bioquímica y Biología Molecular IV, Universidad Complutense, Madrid, Spain

Mouse embryonic stem (ES) glucose-6-phosphate (G6P) dehydrogenase-deleted cells (*G6pdΔ*), obtained by transient Cre recombinase expression in a *G6pd*-loxed cell line, are unable to produce G6P dehydrogenase (G6PD) protein (EC 1.1.1.42). These *G6pdΔ* cells proliferate *in vitro* without special requirements but are extremely sensitive to oxidative stress. Under normal growth conditions, ES *G6pdΔ* cells show a high ratio of NADPH to $NADP^+$ and a normal intracellular level of GSH. In the presence of the thiol scavenger oxidant, azodicarboxylic acid bis[dimethylamide], at concentrations lethal for *G6pdΔ* but not for wild-type ES cells, NADPH and GSH in *G6pdΔ* cells dramatically shift to their oxidized forms. In contrast, wild-type ES cells are able to increase rapidly and intensely the activity of the pentose-phosphate pathway in response to the oxidant. This process, mediated by the [NADPH]/[$NADP^+$] ratio, does not occur in *G6pdΔ* cells. G6PD has been generally considered essential for providing NADPH-reducing power. We now find that other reactions provide the cell with a large fraction of NADPH under non-stress conditions, whereas G6PD is the only NADPH-producing enzyme activated in response to oxidative stress, which can act as a guardian of the cell redox potential. Moreover, bacterial G6PD can substitute for the human enzyme, strongly suggesting that a relatively simple mechanism of enzyme kinetics underlies this phenomenon.

Key words: apoptosis, diamide, GSH, NADPH, thiol.

INTRODUCTION

As a critical modulator of intracellular redox potential, NADPH is the principal source of reducing power in numerous processes of great physiological importance, including the biosynthesis of fatty acids and steroids, detoxification of xenobiotics, defence against oxidative stress and production of nitric oxide [1]. The ratio of reduced to oxidized forms [NADPH]/[$NADP^+$] is close to 10:1 in most cell types [2]. By acting as the electron donor cofactor in the GSH reductase reaction, NADPH is critical in maintaining appropriate levels of GSH, the most abundant source of non-protein thiols. In mammalian cells, the ratio of reduced to oxidized [GSH]/[GSSG] favours the reduced form, although its value varies among the different subcellular compartments. Reported values for [GSH]/[GSSG] are 50–100:1 in the cytosol and 2:1 in the endoplasmic reticulum [3]. Thus, the intracellular levels of two key molecules involved in the control of the cell redox potential are interrelated, with NADPH determining the concentration of GSH.

NADPH is generated by a variety of reactions. It is generally believed that in many cells, including red blood cells (RBC) and hepatocytes, a major part of the NADPH requirement is met by the oxidation of glucose 6-phosphate (G6P) to ribulose 5-phosphate and CO_2 in the pentose-phosphate pathway (PPP) [1]. This is certainly true for RBC, which lack sources of NADPH other than the PPP such that NADPH levels are reduced in human RBC containing low-activity variants of the first and key PPP regulatory enzyme, G6P dehydrogenase (G6PD) (EC 1.1.1.42) [4]. In fact, G6PD deficiency, being the most prevalent enzyme deficiency in man [5], has generated considerable interest and RBC have been the subject of a vast majority of studies on the PPP in recent years. However, the possible contribution of different NADPH sources in nucleated cell types is less clear and is a crucial point in our understanding of the mechanisms controlling redox homoeostasis in mammalian cells.

Targeted gene deletion is a powerful tool in cell metabolism studies, provided the deletion does not remove a function essential for cell survival. Previous work on a mouse embryonic stem (ES) cell line, in which a gene encoding neomycin phosphotransferase gene under the control of the phosphoglycerokinase promoter (NEO cassette) was inserted by homologous recombination into an exon of the *G6pd* gene, revealed that these cells are able to proliferate *in vitro* (although at a reduced rate), have a lower plating efficiency and are extremely sensitive to exogenous oxidative stress [6]. Nevertheless, it was recently shown using the same targeting vector that the ES cell lines produced retain a

Abbreviations used: diamide, azodicarboxylic acid bis[dimethylamide]; ES, embryonic stem; G6P, glucose 6-phosphate; G6PD, G6P dehydrogenase; *G6pdΔ*, *G6pd*-deleted cells; H6PD, hexose-6-phosphate dehydrogenase; Hprt, hypoxanthine–guanine phosphoribosyltransferase; IDH, isocitric dehydrogenase; Mod1, 'malic' enzyme; MTS, [3-(4,5-dimethylthiazol-2-yl)-5-(3-carboxymethoxyphenyl)-2-(4-sulphophenyl)-2*H*-tetrazolium, inner salt]; MTT, 3-(4,5-dimethylthiazol-2-yl)-2,5-diphenyl-2*H*-tetrazolium bromide; NEO cassette, gene encoding neomycin phosphotransferase gene under the control of the phosphoglycerokinase promoter; 6PGD, 6 phospho-gluconate dehydrogenase; PPP, pentose-phosphate pathway; RBC, red blood cells; RT, reverse transcriptase.

[1] To whom correspondence should be addressed (e-mail filosa@iigb.na.cnr.it).

small amount of G6PD activity; thus, these ES cell lines are severely G6PD-deficient rather than G6PD null [7]. To investigate the physiological functions that are dependent on G6PD activity in mammals, we constructed *G6pd*-deleted cells (*G6pdΔ*), a Cre/loxP-based mouse ES cell line bearing a permanent deletion of a *G6pd* exon, critical for enzyme activity. We then analysed the redox potential and antioxidant response of *G6pdΔ* cells in the context of normal *in vitro* growth conditions or in the presence of azodicarboxylic acid bis[dimethylamide] (diamide), a potent oxidant of thiol groups.

MATERIALS AND METHODS

Generation of *G6pdΔ* ES cell lines

Murine *G6pd* clones were isolated from an isogenic 129sv mouse genomic λ library (Stratagene, La Jolla, CA, U.S.A.) by hybridization screening using a mouse cDNA clone [8]. The genomic fragment containing the sequence between part of intron 2 and part of exon 13 was used in the construction of the targeting vector based on pBluescript SK+. The NEO cassette flanked by two flp sites and a loxP site was inserted into the *Bbr*PI site in intron 9; the second loxP site was inserted into intron 10 at a *Bam*HI site generated by site-directed PCR mutagenesis. The targeting vector linearized with *Sal*I was transfected into AK7 ES cells (gift from Dr P. Soriano, Fred Hutchinson Cancer Research Center, Seattle, WA, U.S.A.) and selected with 300 μg/ml of G418. The cells were cultured on neomycin-resistant mouse fibroblasts, as described by Robertson [9]. Resistant colonies were isolated and screened by PCR. The genomic DNA of PCR-positive colonies was digested with *Acc*I restriction endonuclease, fractionated by electrophoresis on 1 % agarose gel in TAE buffer (40 mM Tris/acetate, 10 mM EDTA; pH 8.0), transferred by alkaline capillary blotting to positively charged membranes and hybridized using a probe 3′, external to the targeting sequences. The same filter was hybridized using an internal probe containing the cDNA sequence of exons 9 and 10. Six homologous recombinant flpNEOloxP-positive clones out of 400 were isolated. To generate the *G6pdΔ* ES cell lines, a homologous recombinant flpNEOloxP positive clone was transfected with the plasmid pMCCrePuro (gift from Dr Paul Orban, HSR, Scientific Research Institute, Milan) that contains the genes for Cre recombinase and puromycin resistance as selection markers. Resistant colonies were again isolated and screened by PCR. The genomic DNA was hybridized as mentioned above (Figure 1B).

Two different *G6pdΔ* ES cell lines were used in the experiments described.

For generation of *zwf* (G6PD gene) ES cells, the two *G6pdΔ* ES cell lines were electroporated with 20 μg of linearized plasmid vector Pallino β-actin *Escherichia coli zwf*, a plasmid vector containing *E. coli zwf* (G6PD) cDNA driven by β-actin promoter, and the puromycin resistance gene driven by the phosphoglycerokinase promoter. One week after the selection with 1.2 μg/ml puromycin, the resistant clones were pooled, expanded and subjected to the above-described experiments.

RNA extraction and reverse transcriptase (RT)–PCR

Total cellular RNA was isolated from guanidium isothiocyanate-lysed cells grown on gelatin-coated plates and was purified by acidic phenol extraction [10]. RT–PCR was performed using the PerkinElmer RT–PCR kit, as recommended by the manufacturer. The PCR oligos capable of co-amplifying *G6pd* and the intronless *G6pd-2* were U10-exon 9 (5′-TTGAAGTGTATCTCAGAGGT-GGAA-3′) and L-exon 11 (5′-CAGAAGACATCCAGGATG-AG-3′). The oligos specific for hypoxanthine–guanine phosphoribosyltransferase (Hprt) were U-exon-3-Hprt (5′-CCTGCTGG-ATTACATTAAAGCACTG-3′) and L-exon-8-Hprt (5′-CCTG-AAGTACTCATTATAGTCAAGG-3′).

Immunoblot analysis

Protein extracts prepared from cells grown on gelatin-coated plates were subjected to immunoblot analysis using anti-human-G6PD [11] and anti-ATF2 (activating transcription factor 2; New England Biolabs, Beverly, MA, U.S.A.) antibodies. The cell extracts were separated by SDS/PAGE (10 % gel) and transferred to Immobilon-P transfer membranes (Millipore Corporation, Bedford, MA, U.S.A.). Membranes were blocked with 5 % non-fat milk proteins and incubated with antibodies at a dilution of 1:5000. Bound antibodies were detected by the appropriate horseradish peroxidase-conjugated secondary antibodies followed by ECL® (Amersham).

GSH and GSSG measurements

To determine intracellular levels of GSH and GSSG, acidic extracts from cells untreated or treated for 30 min with 150 μM diamide were subjected to reversed-phase HPLC using an electrochemical detection system. This technique allows extremely sensitive and simultaneous quantification of both GSSG and GSH [12]. The cells grown on gelatin-coated plates were lysed in 5 % metaphosphoric acid [13]. Samples were assayed by HPLC essentially according to a published procedure [12] modified as follows. HPLC analysis was performed using a LC-10AD pump (Shimadzu Italia, Milan, Italy) equipped with a model 7725 injector (Rheodyne, Cotati, CA, U.S.A.) with a 20 μl sample loop. The detector was a Coulochem II instrument (ESA, Chelmsford, MA, U.S.A.) equipped with a guard cell and a dual analytical cell, both with in-line filters. Peak areas were analysed using Class-VP Shimadzu software. Chromatography was performed using a mobile phase of 10 mM NaH_2PO_4 (pH 2.8), containing 2 % methanol at a flow rate of 1 ml/min. Electrode potentials applied by the guard cell, cells 1 and 2 were +1000, +350 and +900 mV respectively. Full-scale output was set at 5 μA for cell 1 and 1 μA for cell 2. GSH and GSSG were identified by their retention time after running a standard enriched sample. Calibration curves, obtained by injecting known amounts of purified standards, were used for quantitative analysis. Standard solutions for GSH (1–100 μM) and GSSG (0.1–7 μM) were prepared freshly in mobile phase with or without 1 mM 2-mercaptoethanol respectively.

$NADP^+$ and NADPH measurements

$NADP^+$ and NADPH were spectrofluorimetrically determined (excitation wavelength, 340 nm; emission wavelength, 460 nm) in acidic and alkaline cell extracts respectively, by monitoring enzyme reactions using GSH reductase or G6PD respectively [14]. Fluorometric units were standardized in each experiment with known concentrations of NADPH and $NADP^+$.

Statistical analysis

Response data were evaluated by the General Linear Model procedure (SAS, 1988; Cary, NC, U.S.A.). An individual culture was the experimental unit for analysis of all data ($n = 3$). Data were analysed as a completely randomized design. In the ANOVA, differences between treatment means were determined by Duncan's multiple-range test. To investigate the effects of different relative amounts of diamide on NADPH and $NADP^+$

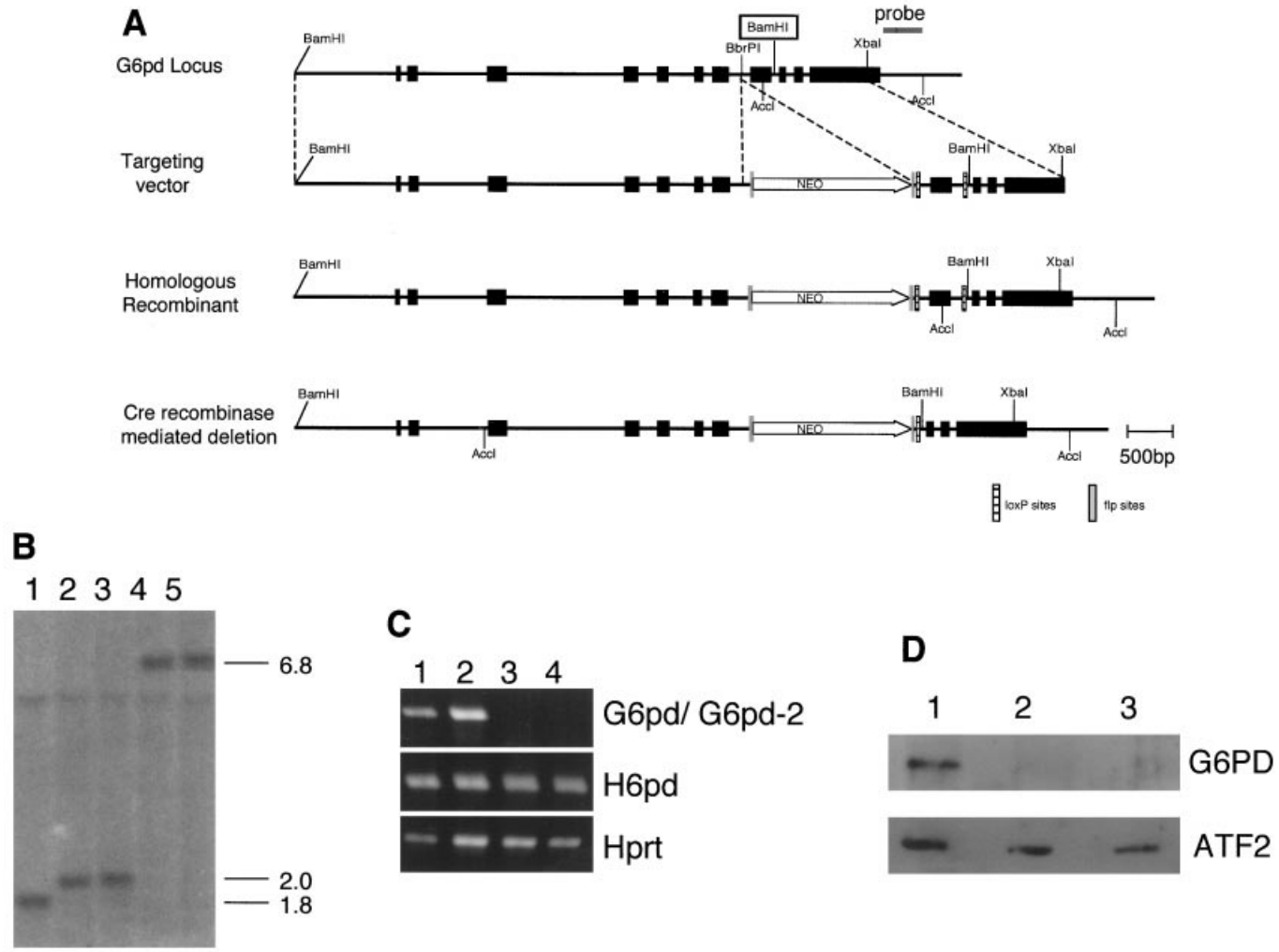

Figure 1 Inactivation of the mouse *G6pd* gene: analysis of RNA and protein production

(**A**) The restriction map of the genomic region containing the *G6pd* gene is shown at the top. Exons (■) and introns (—) are drawn to scale. The *Bam*HI boxed site was inserted by site-directed PCR-mediated mutagenesis. The targeting vector p*G6pd* loxP-flpNEO is shown in the second row; a restriction map of the predicted recombinant loxP *G6pd* allele is shown in the third row; and a restriction map of the *G6pdΔ* allele is shown at the bottom. The probe, which is 3′ external to the genomic sequence of the targeting vector, was used to screen the ES clones. (**B**) Southern-blot analysis. The hybridizing 1.8 kb *Acc*I fragment was derived from the *G6pd*+/Y ES cell line (lane 1). The 2.0 kb *Acc*I fragment was derived from the $G6pd^{loxP-flpNEO}$/Y ES cell line (lanes 2 and 3), and the 6.8 kb *Acc*I fragment from the *G6pdΔ* Y ES cell line (lanes 4 and 5). (**C**) RT–PCR products obtained using primers, which are able to co-amplify *G6pd* and *G6pd*2, and oligos specific for *H6pd* or *Hprt*. Total RNA was isolated from wild-type (lanes 1 and 2) and *G6pdΔ* (lanes 3 and 4) ES cell lines. (**D**) Western-blot analysis. The same filter was probed using anti-G6PD antibodies, stripped and re-probed with antibodies against the ATF2 transcription-factor antibodies. Wild-type (lane 1) and *G6pdΔ* (lanes 2 and 3) cell extracts.

values, means were compared by orthogonal contrasts. Data are provided as the means for each group and pooled standard deviations, together with the significance levels of the main effects and interactions. In all cases, statistical analyses were undertaken using the procedures contained in the SAS software package (version 6.04, SAS Institute, Cary, NC, U.S.A.).

Measurement of $^{14}CO_2$ production

Cells grown in gelatin-coated flasks were preincubated for 1 h in Dulbecco's modified Eagle's medium without sodium pyruvate containing 580 mg/l L-glutamine, 5 mM glucose and 15% dialysed foetal calf serum before the addition of 1 μCi/ml [1-^{14}C]glucose or [6-^{14}C]glucose, or were preincubated for 1 h in Dulbecco's modified Eagle's medium with sodium pyruvate containing 2 mM L-glutamine, 5 mM glucose and 15% dialysed foetal calf serum before the addition of 1 μCi/ml [U-^{14}C]-glutamine. After preincubation, the diamide was added at the concentrations and for the time indicated in Figures 6 and 7. CellTiter96 [50 μl/ml; PMS/3-(4,5-dimethylthiazol-2-yl)-2,5-diphenyl-2*H*-tetrazolium bromide (MTT); Promega] was added to the plates. GSH was added to the cells 30 min before the addition of diamide or PMS/MTT. $^{14}CO_2$ was determined as described in Reitzer et al. [15], modified by benzethonium hydroxide capture of $^{14}CO_2$ [16].

Enzyme activities

Enzyme activities [G6PD, 6 phospho-gluconate dehydrogenase (6PGD), hexose-6-phosphate dehydrogenase (H6PD), Mod I, isocitric dehydrogenase (IDH)] in the whole cell extracts were expressed as m-units/mg of protein at 25 °C. Total protein

concentration was determined using the Bio-Rad Protein Assay Kit (Bio-Rad Laboratories, Hercules, CA, U.S.A.) according to the manufacturer's recommendations.

RESULTS

Generation and characterization of *G6pdΔ* ES cells

Starting from male ES cells, we first produced cell lines in which the *G6pd* exon 10 was flanked by two loxP sites (Figure 1A) by homologous recombination. In these *G6pd-loxed* ES cells, transient expression of Cre recombinase allowed us to obtain cell lines (ES *G6pdΔ* cells) in which exon 10 was ablated by Cre/loxP-mediated site-specific recombination.

Two *G6pd*-deleted ES cell lines were obtained by transient Cre expression and characterized by Southern blotting with an external probe (Figure 1B). The 2.0 kb band, instead of the expected 1.8 kb in wild-type cells, is diagnostic of homologous recombination ($G6pd^{\mathrm{loxP-flpNEO}}$), and a 6.8 kb band should appear when exon 10 is deleted (G6PDΔ). The faint 5.5 kb band, common to all lanes, is due to a mouse-specific intronless gene *G6pd-2*. Southern blotting with a probe internal to the *G6pd* gene showed that the vector was not randomly integrated in the genomic DNA of the clones (results not shown). Using a vector probe, it was verified that the plasmid utilized for transient Cre expression was not integrated in the host genome (results not shown). The two independent *G6pdΔ* cell lines shown in Figure 1 (lanes 4 and 5) were used in all subsequent analyses.

No RT–PCR amplification products were obtained using *G6pd*/*G6pd*-2-specific primers, suggesting that the deletion of exon 10 destabilizes *G6pd* transcripts and that *G6pd*-2, the murine intronless gene *G6pd-2*, is not expressed in ES cells (Figure 1C). Further, we were not able to detect any G6PD-specific immunoreactive products by Western blotting (Figure 1D). However, G6PD-like enzyme activity was observed in extracts from *G6pdΔ* cells, corresponding to 14% of the activity shown by the wild-type cells. This enzyme was able to use G6P or galactose 6-phosphate (Table 1) and is therefore compatible with microsomal H6PD (EC 1.1.1.47) [17], the gene which was recently sequenced [18]. To test if the H6PD gene is expressed in ES cells, we conducted RT–PCR with H6PD-specific primers, and were able to detect H6PD transcripts both in wild-type ES and in *G6pdΔ* cells (Figure 1C).

A comparison of $^{14}CO_2$ production from [1-^{14}C]glucose with $^{14}CO_2$ production from [6-^{14}C]glucose gives an estimate of the flow of glucose carbon through the oxidative arm of the PPP, compared with its entry and cycling in the citric acid cycle. We measured the relative rates of carbon flow through glycolysis and the PPP in wild-type and *G6pdΔ* cells. The results show that most of the glucose is used through the PPP in the wild-type, and that this pathway is completely abolished in *G6pdΔ* cells (Figure 2A). As described before in HeLa cells [15], we also observed that glutamine and not glucose is the major source of energy through the citric acid cycle (Figure 2B) in ES cells. When we determined the relative rates of carbon flow through this pathway using [U-^{14}C]glutamine, no increment was noted in the *G6pdΔ* cells compared with the wild-type cells (Figure 2B).

Table 1 Levels of enzyme activity determined using G6P and NADP

G6pdΔ cells retained traces of an enzyme activity, which was able to catalyse the oxidation of glucose 6-phosphate to 6-phosphogluconate in the presence of coenzyme $NADP^+$. Enzyme activities were determined in whole cell extracts. Each value represents the means ± S.E.M. for three independent determinations.

Cells	G6P (IU/mg of protein)	%	Gal6P (IU/mg of protein)
ES wt	20.9 ± 1.6	100	3.0 ± 0.4
G6pdΔ	3.0 ± 0.3	14	3.0 ± 0.3

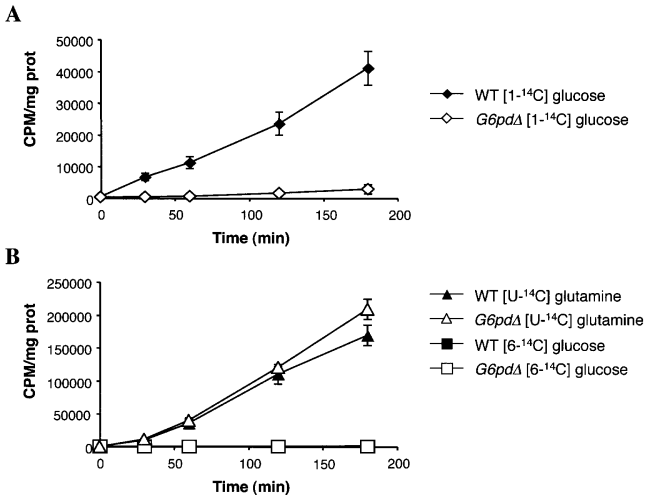

Figure 2 PPP and citric acid cycle activity in wild-type and *G6pdΔ* cell lines

(**A**) Activity of the PPP determined by [1-^{14}C]glucose and the c.p.m./mg of protein of $^{14}CO_2$ released after the indicated time. (**B**) Citric acid cycle activity was determined by treating cells respectively with [6-^{14}C]glucose or [U-^{14}C]glutamine and measuring the c.p.m./mg protein of $^{14}CO_2$ released after the indicated time. Data represent the results for three independent experiments.

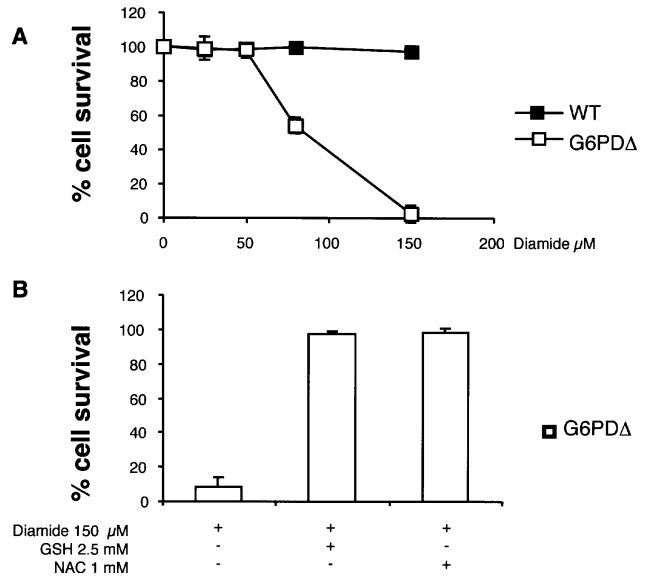

Figure 3 Cell death induced by diamide

(**A**) Diamide-induced cell death in wild-type and *G6pdΔ* cells was evaluated by counting blue cells after Trypan Blue staining. Wild-type and *G6pdΔ* cells were treated with the indicated concentrations of diamide for 3 h. (**B**) *N*-Acetyl-L-cysteine (1 mM) or GSH (2.5 mM), added together with 150 μM diamide, were tested for their ability to rescue *G6pdΔ* cells from death induced in 3 h by the oxidant. The cells were also preincubated for 30 min with 1 mM *N*-acetyl-L-cysteine or 2.5 mM GSH.

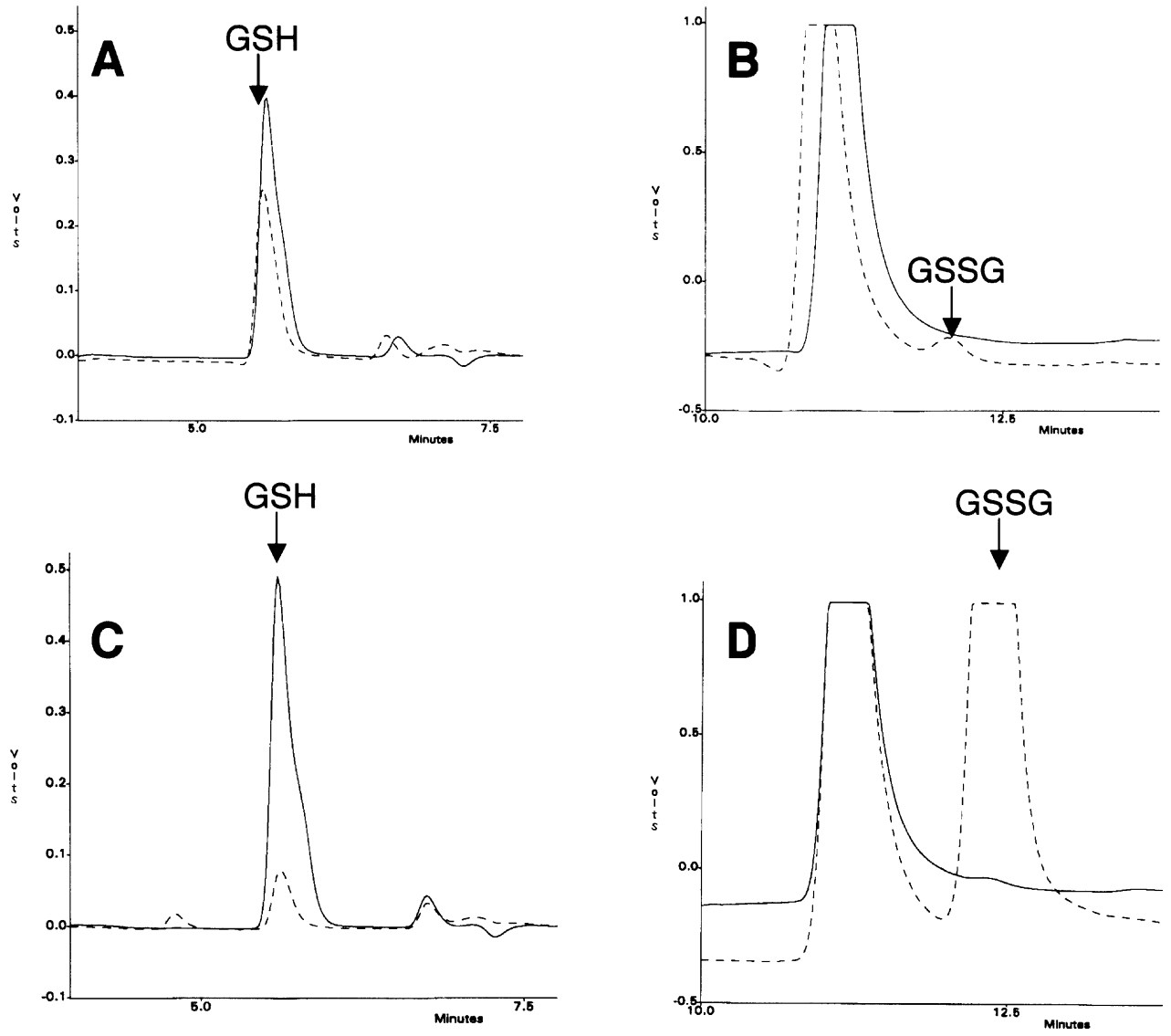

Figure 4 Determination of cellular GSH and GSSG levels by HPLC/electrochemical detection

Representative chromatographic profiles of acid-soluble GSH (**A**, **C**) and GSSG (**B**, **D**) in extracts of wild-type ES cells (**A**, **B**), and *G6pdΔ* ES cells (**C**, **D**) untreated (—) or treated for 30 min with 150 μM diamide (– – –).

Diamide-induced death of *G6pdΔ* cells

To determine the role of G6PD in response to oxidizing agents, we analysed the dose–response curve of *G6pdΔ* cells to diamide (Figure 3A). Exposure for 30 min to diamide concentrations up to 200 μM had no effect on wild-type cells, whereas 80 μM diamide caused the death of 50 % of the *G6pdΔ* cells, and with 150 μM diamide all *G6pdΔ* cells seeded on the experimental plates became Trypan Blue-positive after 16 h. However, in the presence of 2.5 mM GSH or 1 mM *N*-acetyl-L-cysteine in the medium, the *G6pdΔ* cells became resistant to the oxidative stress induced by 150 μM diamide (Figure 3B).

We next examined GSH and GSSG levels in wild-type and *G6pdΔ* cells. In the absence of diamide, *G6pdΔ* cells maintained an intracellular GSH level and a [GSH]/[GSSG] ratio similar to wild-type cells. However, after treatment with 150 μM diamide for 30 min, GSH was oxidized to GSSG and the [GSH]/[GSSG] ratio was dramatically reduced in *G6pdΔ* cells, whereas wild-type cells maintained their normal GSH and GSSG levels (Figure 4 and Table 2).

Under normal culture conditions, $NADP^+$ and NADPH concentrations were not substantially different in the two cell types (Table 3); $NADP^+$ and NADPH levels in wild-type ES cells being in the normal range described for several tissues [19] and *G6pdΔ* cells retaining approx. 90 % of the NADPH shown by the wild-type cells. However, even in the absence of oxidative stress, the *G6pdΔ* cells showed a small deficit of the [NADPH]/[$NADP^+$] ratio compared with the wild-type cells, indicating a limited capacity for maintaining a reduced intracellular environment (Figure 5). After 30 min of exposure to diamide, the [NADPH]/[$NADP^+$] ratio was practically unaltered in wild-type cells, yet oxidized $NADP^+$ increased approx. 4-fold and NADPH decreased accordingly in *G6pdΔ* cells. This increase in $NADP^+$ accompanied by decreasing NADPH resulted in a dramatic

Table 2 GSH and GSSG levels in the presence or absence of 150 μM diamide

GSH and GSSG were determined as described in the Material and methods section. Each value represents the means ± S.E.M. for three independent determinations.

Cells	GSH (nmol/mg)	GSSG (nmol/mg)	GSH/GSSG
WT	33.55 ± 12.41	Undetectable	–
WT + diamide	34.98 ± 17.53	0.24 ± 0.22	222.95 ± 90.56
G6pdΔ	42.96 ± 13.45	0.50 ± 0.26	136.51 ± 128.05
G6pdΔ + diamide	1.34 ± 1.70*	23.21 ± 15.13*	0.29 ± 0.33*

* $P < 0.05$ versus each corresponding control.

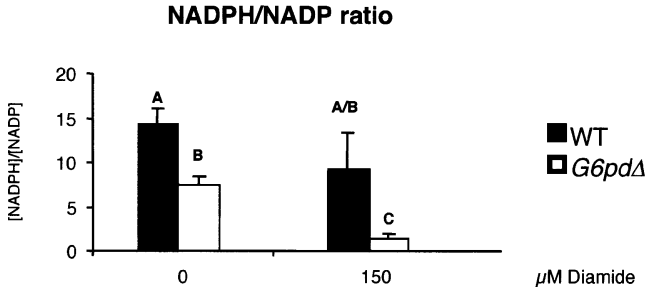

Figure 5 Determination of cellular NADP$^+$ and NADPH contents

Ratio of reduced and oxidized forms of NADP, as determined by the enzymic analysis of cell extracts are shown for untreated cells or cells treated with 150 μM diamide for 30 min. Mean values showing different superscripts were significantly different ($P < 0.05$).

Table 4 Activities of enzymes producing NADPH in the cytoplasm

Enzyme activities were determined in whole cell extracts. Each value represents the means ± S.E.M. for three independent determinations.

Cells	Mod1 (IU/mg of protein)	IDH (IU/mg of protein)	6PGD (IU/mg of protein)
ES wt	9.6 ± 0.8	62.7 ± 1.6	51.4 ± 6.4
G6pdΔ	12.5 ± 3.5	59.5 ± 1.6	52.3 ± 5.6

reduction of the [NADPH]/[NADP$^+$] ratio for *G6pdΔ* cells subjected to oxidative stress (Table 3 and Figure 5). Cytoplasmic NADPH-producing enzymes might be induced in *G6pdΔ* cells to compensate for the absence of G6PD. However, when we measured the activities of 'malic' enzyme (Mod1; EC 1.1.1.40), IDH (EC 1.1.1.42) and 6PGD (EC 4.2.1.12), we observed no differences in the activity of these enzymes between wild-type and *G6pdΔ* cells (Table 4). Moreover, Mod1 and IDH used intermediates of the citric acid cycle as substrates. These substrates are transported into the cytoplasm from the mitochondria and, as shown in Figure 2(B), we noted no increase in the relative rates of carbon flow through the citrate cycle in *G6pdΔ* cells when compared with wild-type cells.

The PPP in ES cells subjected to oxidative stress

A possible explanation for the fact that *G6pdΔ* cells are capable of surviving under normal growth conditions but fail to respond to oxidative insult is that, in the presence of diamide, the PPP needs to be activated for rapid extra NADPH recycling. We therefore determined the amount of $^{14}CO_2$ produced from [1-^{14}C]glucose in wild-type cells grown for 1 h in the presence of diamide and observed intense induction of the PPP (Figure 6A). In contrast, we noted no induction of the citric acid cycle, as determined by [6-^{14}C]glucose or [U-^{14}C]glutamine. Furthermore, the enzyme activities of G6PD and 6PGD shown by cell extracts from wild-type cells treated for 1 h revealed no difference between diamide-treated and control cells (Figure 6B). In addition, no difference in the amount of material immunoreacting with G6PD-specific antibodies was detected by Western blotting (Figure 6C). We also observed that the presence of 2.5 mM GSH in the medium blocked the activation of the PPP by 150 μM diamide (Figure 6A). Analogous experiments performed on *G6pdΔ* cells indicated that neither the PPP nor the citric acid cycle was activated in the presence of diamide (Figure 6A). Finally, we added a NADPH oxidant solution (PMS/MTT), containing a tetrazolium compound, [3-(4,5-dimethylthiazol-2-yl)-5-(3-carboxymethoxyphenyl)-2-(4-sulphophenyl)-2H-tetrazolium, inner salt] (MTS), and an electron-coupling reagent, phenazine ethosulphate, to the ES cell medium. The MTS tetrazolium compound is bioreduced by cells to a coloured formazan product, which is soluble in tissue-culture medium. This reaction is accomplished by conversion of NADPH into NADP$^+$ in the cells. By monitoring the amount of $^{14}CO_2$ produced from [1-^{14}C]glucose, we observed a 10-fold induction of the PPP in wild-type cells kept for 1 h in the presence of PMS/MTS (Figure 7), but no induction was observed in the citric acid cycle, as determined by [6-^{14}C]glucose or [U-^{14}C]glutamine. Also, GSH was unable to counteract the effect of the PMS/MTS. In *G6pdΔ* cells, neither the PPP nor citric acid cycle was activated in the presence of NADPH oxidation (Figure 7). The above results confirm that the PPP is strongly activated in the cells when there is a change in the intracellular [NADPH]/[NADP$^+$] ratio.

To establish the possibility that specific mechanisms evolved with the appearance of multicellular organisms, we then tested whether a bacterial enzyme could substitute for the mouse G6PD in protecting ES cells against oxidative stress. *G6pdΔ* cells were stably transfected with an expression vector containing the *E. coli zwf* (G6PD) gene under the control of the β-actin promoter (*zwf* ES cells). We then compared the amount of $^{14}CO_2$ produced from [1-^{14}C]glucose in *zwf* ES cells grown in the presence of diamide for 1 h, with the amount produced in wild-type cells. The results obtained were identical (Figure 8).

Table 3 NADP levels in the presence or absence of 150 μM diamide

NADPH and NADP$^+$ were determined as described in the Material and methods section. Each value represents the means ± S.E.M. for three independent determinations.

Cells	NADPH (nmol/mg)	NADP$^+$ (nmol/mg)	[NADPH]/[NADP$^+$]
WT	0.14 ± 0.03	0.01 ± 0.001	14.23 ± 3.35
WT + diamide	0.15 ± 0.08	0.02 ± 0.002	9.23 ± 5.84
G6pdΔ	0.13 ± 0.02	0.02 ± 0.003	7.50 ± 1.83
G6pdΔ + diamide	0.09 ± 0.04	0.06 ± 0.015	1.36 ± 0.62

DISCUSSION

Although present in all living cells, most studies on the PPP have been performed in RBC [5]. RBC, however, have simplified biochemical circuits and lack an alternative to the PPP for NADPH production. In other cell types, cytoplasmic NADP$^+$-

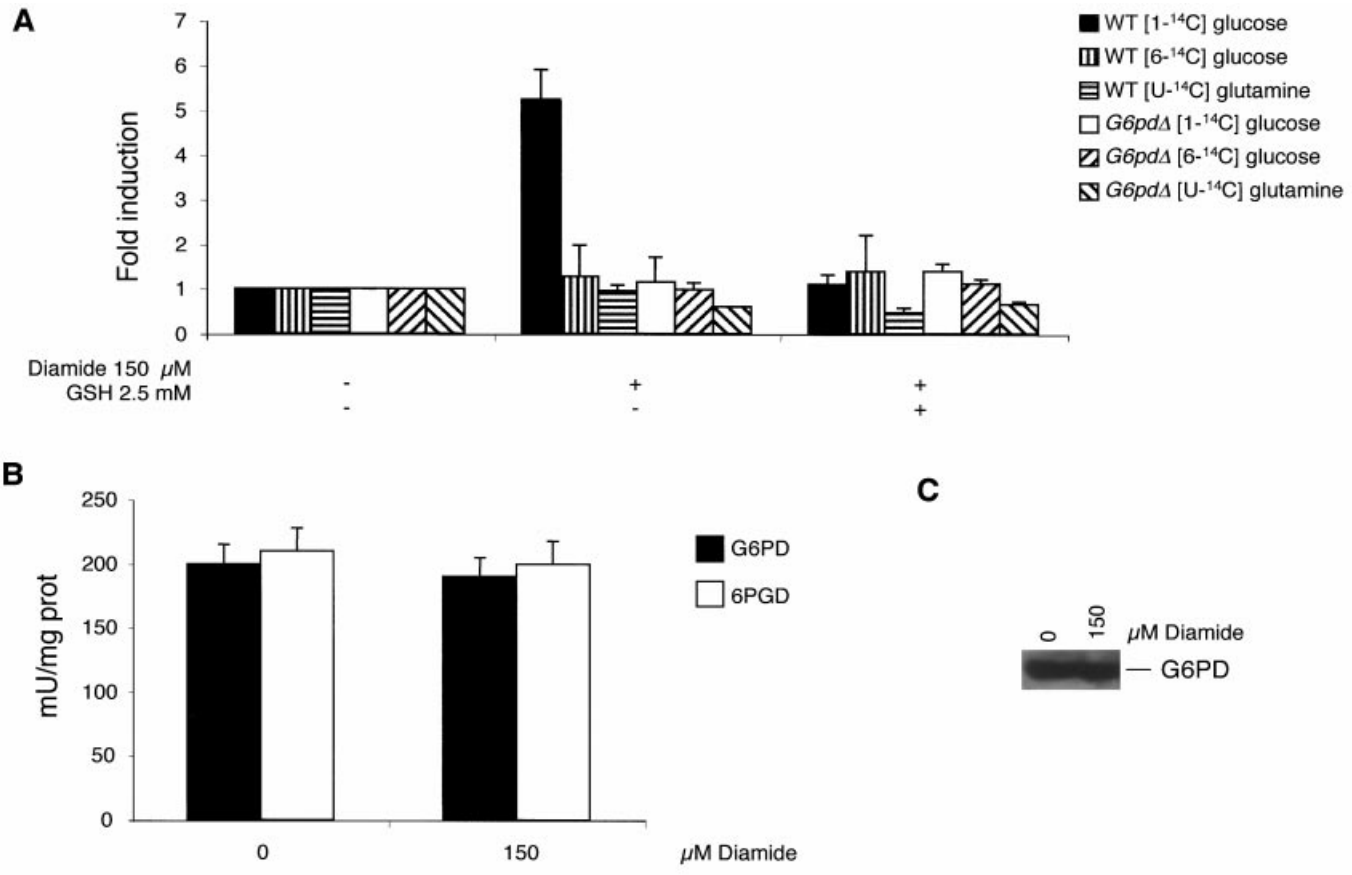

Figure 6 The PPP and citric acid cycle in wild-type ES cells during oxidative stress

(**A**) The induction of the PPP and citric acid cycle, in the presence of 150 μM diamide with or without addition of 2.5 mM GSH, was analysed after 1 h by determining the fold induction with respect to untreated samples. (**B**) G6PD and 6PGD activity in cell extracts. (**C**) Western-blot analysis using the anti-G6PD antibody.

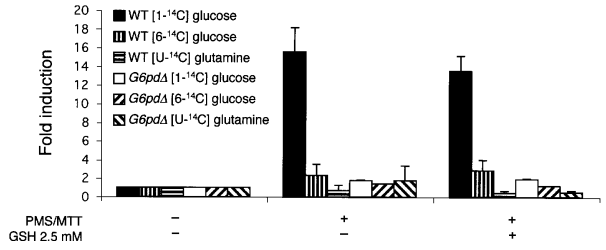

Figure 7 Effect of GSH on the PPP and citric acid cycle in the presence of NADPH oxidant solution (PMS/MTT)

The induction of the PPP and citric acid cycle, in the presence of PMS/MTS with or without 2.5 mM GSH, was analysed by measuring $^{14}CO_2$ released after 1 h, by determining the fold induction with respect to untreated samples.

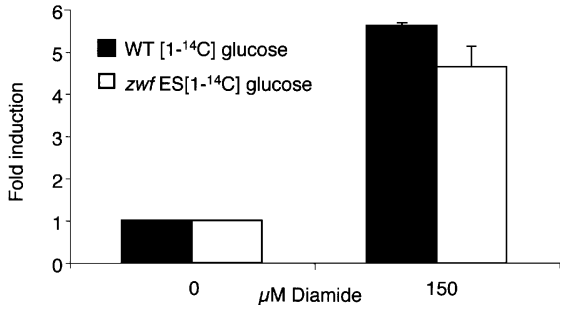

Figure 8 The PPP in *zwf* ES cells during oxidative stress

The activity of the PPP was evaluated by treating cells with 150 μM diamide for 1 h in the presence of [1-^{14}C]glucose. Data are reported as the fold induction with respect to untreated samples.

dependent Mod1 and isocitrate dehydrogenase transfer hydride ions from mitochondrial NADH to cytoplasmic NADP$^+$. Given the key role of NADPH in maintaining redox potentials, clear and detailed knowledge of how NADPH levels are regulated in nucleated cells is of paramount importance [20].

To investigate physiological functions dependent on G6PD activity in mammals and also with the aim to develop a mouse model for tissue-specific analysis, we removed an essential region of the genome, exon 10, by Cre-mediated gene deletion. This gene segment, which encodes a protein domain located at the dimerization interface [21,22], was selected because its deletion could prevent dimerization and enzyme activity. In fact, active G6PD is either a dimer or a tetramer of identical subunits whose equilibrium depends on pH; no enzyme activity is associated with the monomer [23,24]. Furthermore, point mutations in exon

10 generally give rise to highly unstable protein and lead to the severe clinical phenotype of chronic haemolysis [5].

We found that exon 10 deletion destabilizes *G6pd*-specific transcripts such that *G6pd*-specific mRNA, and immunoreactive material are undetectable in *G6pdΔ* cell extracts, probably because the deletion produces an in-frame stop codon downstream (results not shown). Nevertheless, extracts from *G6pdΔ* cells still retained traces of enzyme activity capable of catalysing the oxidation of G6P to 6-phosphogluconate in the presence of the coenzyme $NADP^+$. This residual enzyme activity in *G6pdΔ* cells could use indifferently G6P or galactose-6-phosphate as substrate, a characteristic of the microsomal enzyme H6PD [17,18] which is, in fact, expressed in ES cells. The intronless gene showing testis-specific expression of *G6pd-2*, another potential source of G6PD enzyme in the mouse [25], is not transcribed in ES cells.

Without G6PD, ES cells were able to maintain a high [NADPH]/[$NADP^+$] ratio. There are several possible explanations for the origin of NADPH in *G6pdΔ* cells. First, the H6PD enzyme might substitute for G6PD by feeding the PPP across the microsomal membrane with its phosphogluconate product. Contrary to this hypothesis, we found that the PPP is essentially inactive in *G6pdΔ* cells. Alternatively, Mod1 and IDH, capable of NADPH production, might be up-regulated in the absence of G6PD. However, normal levels of these enzymes were found in *G6pdΔ* cell extracts and it was not possible to detect a large increase in $^{14}CO_2$ production from [6-^{14}C]glucose or [U-^{14}C]glutamine in the *in vivo* analysis of *G6pdΔ* cells, which would be expected if this pathway were active. Our finding that ES *G6pdΔ* cells contain a large fraction of the normal concentration of NADPH thus highlights the importance of pathways that do not depend on G6PD to provide the cell with reducing power in the form of NADPH. It is likely that more than one activity fulfils this role, since mice mutants for the single Mod1 gene appear to have very mild phenotypes [26]. We also noticed that the level of NADPH in *G6pdΔ* cells is sufficient to maintain near-normal levels of GSH.

Reactive oxygen species are capable of inducing the modification of biologically fundamental macromolecules, including the oxidation of GSH and SH groups of protein. Diamide can be considered a reactive oxygen species mimetic, and is in fact an oxidant probe for thiols that are able to penetrate cell membranes within seconds and to react quickly (seconds to minutes) within the cell at physiological pH [27]. This agent has been used in the past to select *G6PD*-expressing heterokaryons and cells in G6PD-deficient backgrounds [28,29], as well as to induce apoptosis in cells of the immune system [30]. When we added diamide to the *G6pdΔ* cell-culture medium, the rate of NADPH recycling was not sufficient to support GSH reduction, and the cells underwent a rapid decrease in NADPH and GSH concentration, leading to their death by apoptosis. It thus appears that G6PD plays a critical role when the cell needs to respond rapidly to exogenous oxidative insult, by replenishing the intracellular pool of GSH. This phenomenon could be easily explained if intense, rapid induction of the PPP is mediated by housekeeping G6PD in response to oxidative stress in a fashion that cannot be duplicated by Mod1 or IDH. In agreement with this hypothesis, we found that within 1 h of adding diamide to wild-type ES cells *in vivo*, the rate of glucose metabolized through the PPP increased more than 6-fold, whereas no induction of the citric acid cycle occurred. We therefore conclude that G6PD is the only NADPH-producing enzyme activated in response to oxidative stress. An increase in G6PD activity in response to a wide range of inducers [31,32], including oxidative stress [33], has also been described previously. However, in these examples the response only occurred after several hours or days, requiring *de novo* enzyme synthesis, and the induction was limited compared with the immediate response of the PPP demonstrated here.

Rapid induction of the PPP in response to oxidative stress can be explained by two mechanisms. Either G6PD senses the oxidized state of the thiol groups in the cell with a positive effect on its enzyme activity, perhaps by forming disulphide bridges within the protein or mixed disulphides with GSH [34], or G6PD senses the change in NADPH and $NADP^+$ concentrations occurring during oxidative stress, as NADPH is rapidly utilized to maintain the reduced state of the cell and $NADP^+$ is generated. To distinguish between these two hypotheses, we treated the cells with PMS/MTS, a substance capable of oxidizing NADPH without interfering with thiol groups in the cells. We found that PMS/MTS was able to activate the PPP, even in the presence of excess GSH. Moreover, G6PD-specific activity measured *in vitro* and the amount of material reacting with G6PD-specific antibodies remained unaltered after the diamide insult, suggesting no protein structure modification responsible for enzyme activation. Hence, G6PD activation appears to be determined by [NADPH]–[$NADP^+$] conversion.

It has been reported that $NADP^+$ is not only a G6PD substrate, but is also required to stabilize the dimeric functional form of G6PD [35,36]. In fact, a secondary, structural binding site for $NADP^+$ (different from the enzyme's active site) was revealed in the three-dimensional structure of human G6PD, close to the dimer interface [22] in an area that is 100 % identical in mice and humans. Accordingly, point mutations primarily affecting the stability of the molecule and occurring close to this 'structural' $NADP^+$-binding site are *in vitro* reactivated by increasing the $NADP^+$ concentration [37]. We were able to test if $NADP^+$ binding at the secondary site is necessary for PPP activation following oxidative stress by exploiting the fact that bacterial G6PD enzymes can form dimers without interacting with $NADP^+$ at the dimer interface; in fact they lack a 'structural' $NADP^+$-binding site [22]. The results from the *zwf* ES cells indicate that the bacterial enzyme is able to substitute for the mouse enzyme in activating the PPP under conditions of oxidative stress. Thus, it seems that the newly evolved structural binding site for $NADP^+$, essential for stabilizing the enzyme's quaternary structure, is not an absolute requirement for the rapid increase in PPP activity that occurs in response to oxidative stress or that this binding site is used for some fine-tuning is not revealed by the present analysis.

The formation of mixed disulphides between GSH and cysteines in the proteins (glutathionylation) has been suggested as the mechanism by which protein function can be regulated by redox status [34,38]. In particular, glyceraldehyde-3-phosphate dehydrogenase activity has been reported to be decreased by glutathionylation [34,39]. As a consequence, during oxidative stress, inhibition of the glycolytic pathway makes more G6P available for the PPP, suggesting a simple mechanism for the unique role for G6PD in cell response to oxidative stress. Indeed, known enzyme kinetic parameters and intracellular substrate concentrations lead us to hypothesize that G6PD works at low efficiency under normal cell conditions. When $NADP^+$ is provided (e.g. by consumption of NADPH due to oxidative stress), G6PD will immediately start recycling it to NADPH, thereby increasing glucose consumption.

Glucose has been ascribed an essential role in protecting cells from apoptosis [40,41]. The enzyme hexokinase is immediately upstream from G6PD, and catalyses the conversion of glucose into G6P. Recent results show that hexokinase is able to attenuate apoptosis in a glucose-dependent manner [42,43]. Our results suggest an important role for G6PD, as a downstream effector of

hexokinase, in protecting cells from oxidative stress-induced apoptosis.

We thank P. H. Byers, J. Guardiola, E. Patriarca and I. Iaccarino for critical reading of the manuscript; P. Soriano for kindly providing the ES cells; P. Orban for kindly providing the pMC-CREPuro plasmid construct; G. Minchiotti and S. Parisi for kindly providing the Pallino βactin vector; C. Lopez Bote (UCM, Madrid) for help with the statistical analysis; M. Terracciano and R. Vito for their skilful laboratory assistance; and C. Rallo, M. Petrillo and S. Cossu for help with the computer. This work was supported by the Italian Telethon Foundation, grant no. 324/bi and Progetto Ministero dell'Università e della Ricerca Scientificae Tecnologica–Il Consiglio Nazionale delle Ricerche Legge 488/92 (Cluster C02).

REFERENCES

1 Stryer, L. (1995) Biochemistry, Freeman W. H. and company, New York
2 Halliwell, B. and Gutteridge, J. M. C. (1999) Free Radicals in Biology and Medicine, Oxford University Press, New York
3 Hwang, C., Sinskey, A. J. and Lodish, H. F. (1992) Oxidised redox state of glutathione in the endoplasmic reticulum. Science **257**, 1496–1502
4 Mareni, C. and Gaetani, G. F. (1976) $NADP^+$ and NADPH in glucose-6-phosphate dehydrogenase-deficient erythrocytes under oxidative stimulation. Biochim. Biophys. Acta **430**, 395–398
5 Luzzatto, L. and Mehta, A. (1988) Glucose-6-phosphate dehydrogenase deficiency, in The Metabolic Basis of Inherited Disease, pp. 2237–2265, McGraw-Hill, New York
6 Pandolfi, P. P., Sonati, F., Rivi, R., Mason, P., Grosveld, F. and Luzzatto, L. (1995) Targeted disruption of the housekeeping gene encoding glucose 6-phosphate dehydrogenase (G6PD): G6PD is dispensable for pentose synthesis but essential for defense against oxidative stress. EMBO J. **14**, 5209–5215
7 Longo, L., Vanegas, O. C., Patel, M., Rosti, V., Li, H., Waka, J., Merghoub, T., Pandolfi, P. P., Notaro, R., Manova, K. et al. (2002) Maternally transmitted severe glucose 6-phosphate dehydrogenase deficiency is an embryonic lethal. EMBO J. **21**, 4229–4239
8 Zollo, M., D'Urso, M., Schlessinger, D. and Chen, E. Y. (1993) Sequence of mouse glucose-6-phosphate dehydrogenase cDNA. DNA Seq. **3**, 319–322
9 Robertson, E. J. (1987) Embryo-derived stem cell lines. In Teratocarcinomes and Embryonic Stem Cells: A Particle Approach (Robertson, E. J., ed.), pp. 71–112, IRL Press, Oxford
10 Chomczynski, P. and Sacchi, N. (1987) Single-step method of RNA isolation by acid guanidinium thiocyanate–phenol–chloroform extraction. Anal. Biochem. **162**, 156–159
11 Gomez Gallego, F., Garrido Pertierra, A., Mason, P. J. and Bautista, J. M. (1996) Unproductive folding of the human G6PD-deficient variant A. FASEB J. **10**, 153–158
12 Smith, N. C., Dunnett, M. and Mills, P. C. (1995) Simultaneous quantitation of oxidised and reduced glutathione in equine biological fluids by reversed-phase high-performance liquid chromatography using electrochemical detection. J. Chromatogr. B. **673**, 35–41
13 Shi, Z. Z., Osei Frimpong, J., Kala, G., Kala, S. V., Barrios, R. J., Habib, G. M., Lukin, D. J., Danney, C. M., Matzuk, M. M. and Lieberman, M. W. (2000) Glutathione synthesis is essential for mouse development but not for cell growth in culture. Proc. Natl. Acad. Sci. U.S.A. **97**, 5101–5106
14 Klingenberg, M. (1974) Nicotinamide-adenine dinucleotides. Spectrophotometric and Fluorimetric methods, in Methods of Enzymatic Analysis, vol. 4 (Bergmeyer, H. U., ed.), pp. 2045–2059, Verlag Chemie GmbH, Weinheim
15 Reitzer, L. J., Wice, B. M. and Kennell, D. (1979) Evidence that glutamine, not sugar, is the major energy source for cultured HeLa cells. J. Biol. Chem. **254**, 2669–2676
16 Delicado, E., Torres, M. and Miras Portugal, M. T. (1986) Effects of insulin on glucose transporters and metabolic patterns in Harding–Passey melanoma cells. Cancer Res. **46**, 3762–3767
17 Ohno, S., Payne, H. W., Morrison, M. and Beutler, E. (1966) Hexose-6-phosphate dehydrogenase found in human liver. Science **153**, 1015–1016
18 Mason, P. J., Stevens, D., Diez, A., Knight, S. W., Scopes, D. A. and Vulliamy, T. J. (1999) Human hexose-6-phosphate dehydrogenase (glucose 1-dehydrogenase) encoded at 1p36: coding sequence and expression. Blood Cells Mol. Dis. **25**, 30–37
19 Williamson, J. R. and Corkey, B. E. (1969) Assays of intermediates of the citric acid cycle and related compounds by fluorimetric enzyme methods. Methods Enzymol. **XIII**, 434–513
20 Martini, G. and Ursini, M. V. (1996) A new lease of life for an old enzyme. Bioessays **18**, 631–637
21 Naylor, C. E., Rowland, P., Basak, A. K., Gover, S., Mason, P. J., Bautista, J. M., Vulliamy, T. J., Luzzatto, L. and Adams, M. J. (1996) Glucose 6-phosphate dehydrogenase mutations causing enzyme deficiency in a model of the tertiary structure of the human enzyme. Blood **87**, 2974–2982
22 Au, S. W., Gover, S., Lam, V. M. and Adams, M. J. (2000) Human glucose-6-phosphate dehydrogenase: the crystal structure reveals a structural NADP(+) molecule and provides insights into enzyme deficiency. Struct. Fold. Des. **8**, 293–303
23 Cohen, P. and Rosemeyer, M. A. (1969) Human glucose-6-phosphate dehydrogenase: purification of the erythrocyte enzyme and the influence of ions on its activity. Eur. J. Biochem. **8**, 1–7
24 Babalola, A. O., Beetlestone, J. G. and Luzzatto, L. (1976) Genetic variants of human erythrocyte glucose-6-phosphate dehydrogenase. Kinetic and thermodynamic parameters of variants A, B, and A- in relation to quaternary structure. J. Biol. Chem. **251**, 2993–3002
25 Hendriksen, P. J. M., Hoogerbrugge, J. W., Baarends, W. M., De Boer, P., Vreeburg, J. T. M., Vos, E. A., Van Der Lende, T. and Grootegoed, J. A. (1997) Testis-specific expression of a functional retroposon encoding glucose-6-phosphate dehydrogenase in the mouse. Genomics **41**, 350–359
26 Lee, C. Y., Chasalow, F., Lee, S. M., Lewis, S. and Johnson, F. M. (1980) A null mutation of cytoplasmic malic enzyme in mice. Mol. Cell. Biochem. **30**, 143–149
27 Kosower, N. S. and Kosower, E. M. (1995) Diamide: an oxidant probe for thiols. Methods Enzymol. **251**, 123–133
28 D'Urso, M., Mareni, C., Toniolo, D., Piscopo, M., Schlessinger, D. and Luzzatto, L. (1983) Regulation of glucose-6-phosphate dehydrogenase expression in CHO-human fibroblast somatic cell hybrids. Somat. Cell Genet. **9**, 429–443
29 Warren, S. T., Zhang, F., Licameli, G. R. and Peters, J. F. (1987) The fragile X site in somatic cell hybrids: an approach for molecular cloning of fragile sites. Science **237**, 420–423
30 Sato, N., Iwata, S., Nakamura, K., Hori, T., Mori, K. and Yodoi, J. (1995) Thiol-mediated redox regulation of apoptosis. Possible roles of cellular thiols other than glutathione in T cell apoptosis. J. Immunol. **154**, 3194–3203
31 Kletzien, R. F., Harris, P. K. and Foellmi, L. A. (1994) Glucose-6-phosphate dehydrogenase: a 'housekeeping' enzyme subject to tissue-specific regulation by hormones, nutrients, and oxidant stress. FASEB J. **8**, 174–181
32 Preville, X., Salvemini, F., Giraud, S., Chaufour, S., Paul, C., Stepien, G., Ursini, M. V. and Arrigo, A. P. (1999) Mammalian small stress proteins protect against oxidative stress through their ability to increase glucose-6-phosphate dehydrogenase activity and by maintaining optimal cellular detoxifying machinery. Exp. Cell Res. **247**, 61–78
33 Ursini, M. V., Parrella, A., Rosa, G., Salzano, S. and Martini, G. (1997) Enhanced expression of glucose-6-phosphate dehydrogenase in human cells sustaining oxidative stress. Biochem. J. **323**, 801–806
34 Fratelli, M., Demol, H., Puype, M., Casagrande, S., Eberini, I., Salmona, M., Bonetto, V., Mengozzi, M., Duffieux, F., Miclet, E. et al. (2002) Identification by redox proteomics of glutathionylated proteins in oxidatively stressed human T lymphocytes. Proc. Natl. Acad. Sci. U.S.A. **99**, 3505–3510
35 Cancedda, R., Ogunmola, G. and Luzzatto, L. (1973) Genetic variants of human erythrocyte glucose-6-phosphate dehydrogenase. Discrete conformational states stabilized by NADP+ and NADPH. Eur. J. Biochem. **34**, 199–204
36 Scopes, D. A., Bautista, J. M., Naylor, C. E., Adams, M. J. and Mason, P. J. (1998) Amino acid substitutions at the dimer interface of human glucose-6-phosphate dehydrogenase that increase thermostability and reduce the stabilising effect of NADP. Eur. J. Biochem. **251**, 382–388
37 Hirono, A., Kuhl, W., Gelbart, T., Forman, L., Fairbanks, V. F. and Beutler, E. (1989) Identification of the binding domain for NADP+ of human glucose-6-phosphate dehydrogenase by sequence analysis of mutants. Proc. Natl. Acad. Sci. U.S.A. **86**, 10015–10017
38 Casagrande, S., Bonetto, V., Fratelli, M., Gianazza, E., Eberini, I., Massignan, T., Salmona, M., Chang, G., Holmgren, A. and Ghezzi, P. (2002) Glutathionylation of human thioredoxin: a possible crosstalk between the glutathione and thioredoxin systems. Proc. Natl. Acad. Sci. U.S.A. **99**, 9745–9749
39 Ravichandran, V., Seres, T., Moriguchi, T., Thomas, J. A. and Johnston, R. B. J. (1994) S-thiolation of glyceraldehyde-3-phosphate dehydrogenase induced by the phagocytosis-associated respiratory burst in blood monocytes. J. Biol. Chem. **269**, 25010–25015
40 Moley, K. H. and Mueckler, M. M. (2000) Glucose transport and apoptosis. Apoptosis **5**, 99–105
41 Vander Heiden, M. G., Plas, D. R., Rathmell, J. C., Fox, C. J., Harris, M. H. and Thompson, C. B. (2001) Growth factors can influence cell growth and survival through effects on glucose metabolism. Mol. Cell. Biol. **21**, 5899–5912
42 Gottlob, K., Majewski, N., Kennedy, S., Kandel, E., Robey, R. B. and Hay, N. (2001) Inhibition of early apoptotic events by Akt/PKB is dependent on the first committed step of glycolysis and mitochondrial hexokinase. Genes Dev. **15**, 1406–1418
43 Pastorino, J. G., Shulga, N. and Hoek, J. B. (2002) Mitochondrial binding of hexokinase II inhibits Bax-induced cytochrome *c* release and apoptosis. J. Biol. Chem. **277**, 7610–7618

Received 16 October 2002/4 December 2002; accepted 4 December 2002
Published as BJ Immediate Publication 4 December 2002, DOI 10.1042/BJ20021614